

Poly (*N*-methylaniline)/Multi-Walled Carbon Nanotube Composites—Synthesis, Characterization, and Electrical Properties

Xiaofeng Lu,¹ Jiani Zheng,¹ Danming Chao,¹ Jingyu Chen,¹ Wanjin Zhang,¹ Yen Wei²

¹Alan G. MacDiarmid Institute, Jilin University, Changchun 130012, People's Republic of China

²Department of Chemistry, Drexel University, Philadelphia, Pennsylvania 19104

Received 17 July 2005; accepted 29 August 2005

DOI 10.1002/app.23068

Published online in Wiley InterScience (www.interscience.wiley.com).

ABSTRACT: This study described the synthesis of hydrochloric acid (HCl)-doped poly (*N*-methylaniline) (PNMA) with carboxylic groups containing multi-walled carbon nanotubes (c-MWNTs) via in situ polymerization. Based on the π - π electron interaction between c-MWNTs and the *N*-methylaniline monomer and the hydrogen bond interaction between the carboxyl groups of c-MWNTs and imine groups of *N*-methylaniline monomers, *N*-methylaniline molecules were adsorbed on the surface of c-MWNTs and polymerized to form PNMA/c-MWNT composites. Scanning electron microscopy images showed that both the thinner fibrous phase and the larger block phase could be observed. The individual fibrous phases had diameters from several

tens to hundreds of nanometers, depending on the PNMA content. Transmission electron microscopy proved that PNMA/c-MWNTs composite fibrous phases were core (c-MWNT)-shell (PNMA) tubular structures. The structure of PNMA/c-MWNT composites was characterized by FTIR, UV-vis spectra, and X-ray diffraction patterns. The electrical conductivities of PNMA/c-MWNT composites were much higher than that of PNMA without c-MWNTs. © 2006 Wiley Periodicals, Inc. *J Appl Polym Sci* 100: 2356–2361, 2006

Key words: poly (*N*-methylaniline); multi-walled carbon nanotubes; core-shell tubular structures; electrical conductivities

INTRODUCTION

Polyaniline (PANI) became well-known in the past decades because of its useful electronic, photonic, and electroluminescence properties.¹ It has been extensively studied in electrode material, microelectronics, electrochromic material, radiation shielding, and recordable optical discs.^{1–5} However, the major disadvantage of PANI is its insolubility in common organic solvents and its infusibility because of the stiffness of the PANI backbone and the hydrogen-bonding interactions between the amine moieties of adjacent chains. There are some possible methods such as doping various organic acids or copolymerizing of aniline with its derivatives for preparing soluble PANI.^{6–8} Often, the solubilization of a polymer can be achieved through substituting one or more hydrogens by an

alkyl, an alkoxy, an aryl hydroxyl, an amino group, or halogen in an aniline nucleus.^{9–12} However, the lower electrical conductivity limits its wide usage. For example, poly (2-chloroaniline) (P2ClAn) synthesized by Kang and Yun has a conductivity of 7.9×10^{-5} S/cm, whereas that of poly(2-flouroaniline) (P2FAn) is 8.3×10^{-6} S/cm.¹³

Poly (*N*-methylaniline), PNMA, a polymer of an *N*-substituted polyaniline derivative, has been polymerized by electrochemical and chemical polymerization method.^{14–15} Recently, PNMA is found to possess different chemical properties from PANI because of the blocking of protonation sites by the *N*-substituted methyl groups. The deprotonation of the imine group occurring during the second oxidation process of PANI is probably suppressed for PNMA. This suppression reduces the risk of oxidative deterioration by hydrolysis during the electrochemical oxidation, which is superior to PANI.^{16,17} And the polymers can be promising for applications in conductometric sensors, gas sensors, and in potentiometry.^{18–20} So synthesis of PNMA in the processable form becomes essential. Thus the low electrical conductivity limited its being widely used.

In this paper, we describe a relatively high electrical conductivity of PNMA obtained through combining carbon nanotubes (CNT). As we all know, carbon nanotubes have demonstrated a wealth of exceptional

Correspondence to: W. J. Zhang (wjzhang@jlu.edu.cn).

Contract grant sponsor: The Major International Collaborative Project of National Natural Science Foundation of China; contract grant number: 20320120169.

Contract grant sponsor: The National Major Project for Fundamental Research of China; contract grant numbers: National 973 Program No. 001CB610505 and No. G2003CB615604.

Contract grant sponsor: The National Nature Science Foundation of China; contract grant number: 50473007.

electrical, mechanical and thermal properties, which have made them useful for potential applications ranging from nanoelectronics to biomedical devices.^{21,22} The formation of carbon nanotube /polymer composites has been explored for possible improvement in the electrical and mechanical properties of polymers.^{23,24} In particular, composite materials based on the coupling of conducting polymers and CNTs have been shown to possess properties of the individual components with a synergistic effect.²⁵ PANI/CNT and Polypyrrole(PPy)/CNT composites were both widely studied.^{26,27} Here we describe the synthesis of PNMA/CNT composites of high electrical conductivity by *in situ* chemical oxidative polymerization. The electrical conductivity of PNMA/CNT (10 wt % c-MWNT) at room temperature is about 3.7×10^{-3} S/cm, while that of PNMA is only about 1.4×10^{-6} S/cm in the same conditions.

EXPERIMENTAL

Synthesis of PNMA/c-MWNT composites

N-methylaniline monomer was purchased from Nankai University Fine Chemical Lab (China). Multi-walled carbon nanotubes used in this work were purchased from Shenzhen Nanotech Port Co., Ltd (China). Other reagents were used without further purification. The as-prepared MWNTs were treated in a 6M HNO₃ solution using reflux for 12 h, which produced carboxylic acid (—COOH) functional groups at the defect sites (designated as c-MWNTs). The carboxylic acid groups were identified by Fourier transform infrared (FTIR) spectroscopy, similar to that of the others reported before.²⁸

PNMA/c-MWNT composites were synthesized by *in situ* chemical oxidative polymerization. In a typical composite synthesis experiment, various weight ratios of c-MWNTs were dissolved in 80 mL 1M hydrochloric acid solutions and ultrasonicated over 2 h, then transferred into a 250 mL beaker. 0.428 g *N*-methylaniline monomer was added to the above c-MWNTs suspension. Then a 20 mL 1M hydrochloric acid solution containing 0.912 g ammonium persulfate (APS) was added into the suspension with constant mechanical stirring at room temperature. The reaction mixture was stirred for a further 6 h, and then filtered. The remaining filter cake was rinsed several times with distilled water and ethanol. The powder thus obtained was dried under vacuum at 60°C for 24 h.

Measurements

FTIR Spectra of KBr powder-pressed pellets were recorded on a BRUKER VECTOR22 Spectrometer. Transmission spectrum of POT/c-MWNTs was recorded on a Shimadzu UV-2501 PC Spectrometer. X-

ray diffraction patterns (XRD) were obtained with a Siemens D5005 diffractometer using Cu K α radiation. Scanning electron microscopy (SEM) measurements were performed on a SHIMADZU SSX-550 microscope. Transmission electron microscopy (TEM) experiments were performed on a Hitachi 8100 electron microscope (Tokyo, Japan) with an acceleration voltage of 200 kV. The standard Van Der Pauw DC four-probe method²⁹ was used to measure the electron transport behavior of PNMA, PNMA/c-MWNT composites. The samples of PNMA and PNMA/c-MWNTs were pressed into pellet. Then the pellet was cut into a square. The square was placed on the four-probe apparatus. Providing a voltage, a corresponding electrical current could be obtained. The electrical conductivity of samples was calculated by the following formula: σ (S/cm) = $(2.44 \times 10/S) \times (I/E)$, where σ is the conductivity; S is the sample side area; I is the current passed through outer probes; E is the voltage drop across inner probes.

RESULTS AND DISCUSSION

MWNTs (c-MWNTs) with modified carboxylic acid (—COOH) functional groups were synthesized based on the previous report and characterized by FTIR spectrum. Compared with the spectrum of MWNT, the new peaks at around 1717 and 1195 cm⁻¹ apparently corresponding to the stretching modes of the carboxylic acid groups in c-MWNTs were observed.²⁸ This result indicated the formation of carboxylic acid groups on the surface defects of c-MWNTs. As we all know, the HCl-doped PANI is insoluble in most common solvents, while our doped PNMA/c-MWNT composite is soluble in numerous solvents such as acetonitrile (CH₃CN), *N*-methylpyrrolidinone (NMP), and dimethylformamide (DMF). This practical property of PNMA/c-MWNT composite can be used to prepare solution-cast films. The morphology of the resulting PNMA/c-MWNT composites was characterized by SEM and TEM. SEM images clearly showed that there were two different types of material to be visible: the thinner fibrous phase and the larger block phase. With the increasing of c-MWNTs, more and more individual fibrous phases were formed (Fig. 3). The diameters of the individual fibrous phases ranged from several tens to hundreds of nanometers, depending on the PNMA content. The diameters of the individual fibrous phases became larger than that of the original c-MWNTs (diameter 20–30 nm) after *in situ* polymerization, and therefore the carbon nanotubes must be coated by a PNMA layer. The block phases are believed to be PNMA doped by the acid anion. This result can be also proved by TEM. Figure 2 shows the TEM image of the individual fibrous phases of PNMA/c-MWNTs containing 10 wt % c-MWNTs. From it we can clearly observe that PNMA/c-MWNTs

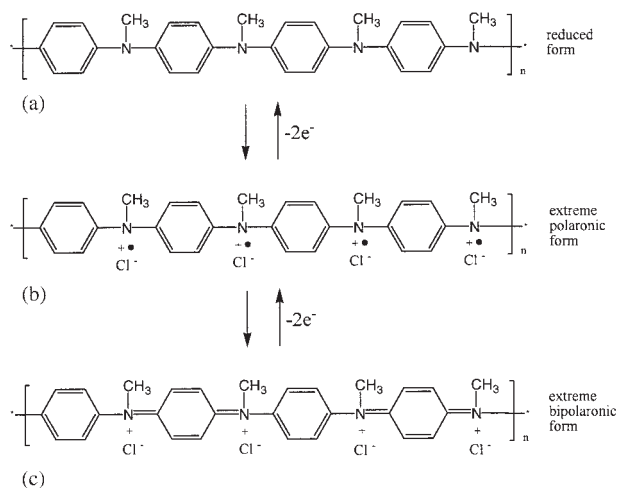


Figure 1 Three different redox forms of PNMA: (a) reduced form, (b) extreme polaronic form, and (c) extreme bipolaronic form.

composite fibrous phases have coaxially tubular structures. This PNMA/c-MWNT composite is the typical core-shell structure, and the c-MWNT serves as the core and is dispersed individually into the PNMA matrices.

The formation mechanism of fibrous phase composite is believed to arise from the weak interaction between PNMA monomer and c-MWNTs. The interaction possibly involves the π - π electron interaction between c-MWNTs and the PNMA monomer and the hydrogen bond interaction between the carboxyl groups of c-MWNTs and imine groups of *N*-methylaniline (or oligomers). Such interactions are ensured by *N*-methylaniline monomer adsorbed on the surface of c-MWNT during the formation of fibrous phase composite. c-MWNTs therefore serve as the template and the core during the formation of the fibrous phase composites, which is similar to the formation of PANI/c-MWNT composites with tubular nanostructure.²⁸

FTIR spectra are used to characterize the structure of PNMA and PNMA/c-MWNT composites, which are presented in Figure 4. For PNMA, the characteristic bands at about 2918 cm^{-1} can be assigned to the stretching vibration of the methyl ($-\text{CH}_3$) group. The two bands at around 1500 and 1577 cm^{-1} are assigned to the stretching vibration of the benzenoid and quinoid ring, respectively.³⁰ The band at 1316 cm^{-1} can be assigned to the C—N vibration. The presence of the band appearing at 822 cm^{-1} is characteristic of the C—H out-of-plane bending vibrations of the *para*-substituted benzene ring. This latter observation confirms the expected head-to-tail coupling polymerization at the C-4 and N positions for PNMA. All of these data are similar to the spectra of PNMA salts, which confirm that the obtained sample is in its doped phase.¹⁴

Clearly, the FTIR spectra of PNMA/c-MWNT composites are almost identical to that of PNMA, indicating that *N*-methylaniline is polymerized on the surface of c-MWNTs to form PNMA/c-MWNT composites. Figure 5 presents the XRD data for PNMA and PNMA/c-MWNT composites. For PNMA, the X-ray scattering patterns exhibit them as amorphous, while PNMA/c-MWNT composites have relatively good crystalline structure than do PNMA. With the increasing of c-MWNTs, new diffraction peaks at $2\theta = 25.9$ and 43° attributed to c-MWNTs patterns are observed, indicating c-MWNTs are as a core in the composites.

The UV-visible spectra of the PNMA/c-MWNTs in NMP solutions are presented in Figure 6. As for the alkalescence of NMP, the spectra are similar with that of emeraldine base of PNMA. The major peak at about 324 and 615 nm is observed, which is assigned to the excitation of the benzene and quinoid segments on the polyemeraldine chain, respectively. To obtain the doped PNMA/c-MWNTs, one drop of 35 wt % HCl is added to the above solutions. The absorption peaks at 320 , 434 , and $\sim 1100\text{ nm}$ are formed, producing five lines of Figure 6. The absorption peak at about 320 nm can be ascribed to π - π^* transition of the benzenoid rings, whereas the peaks at around 410 nm and 1100 nm can be attributed to polaron- π^* and π -polaron transition, following the classical Figure 1.

The electrical conductivities of PNMA and PNMA/c-MWNT composites are measured using the standard Van Der Pauw DC four-probe method. The conductivity of PNMA synthesized in the presence of HCl shows a room temperature conductivity of 1.43×10^{-6}

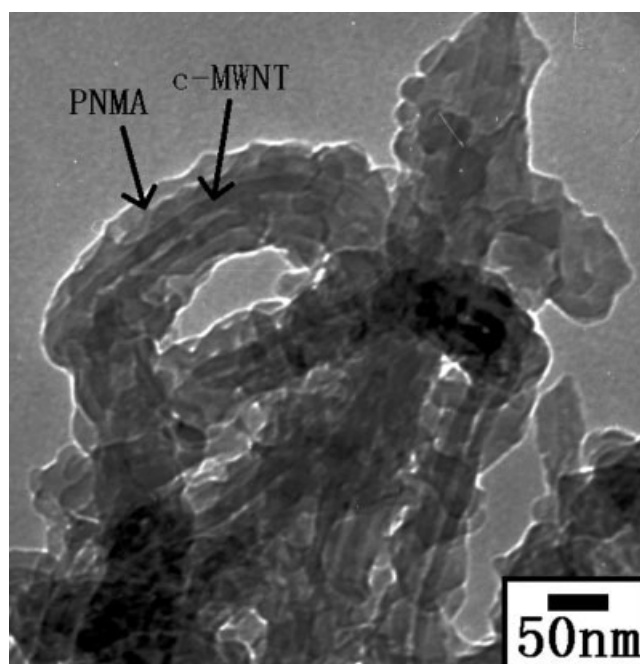


Figure 2 TEM image of 10 wt % c-MWNTs containing PNMA/c-MWNT composite.

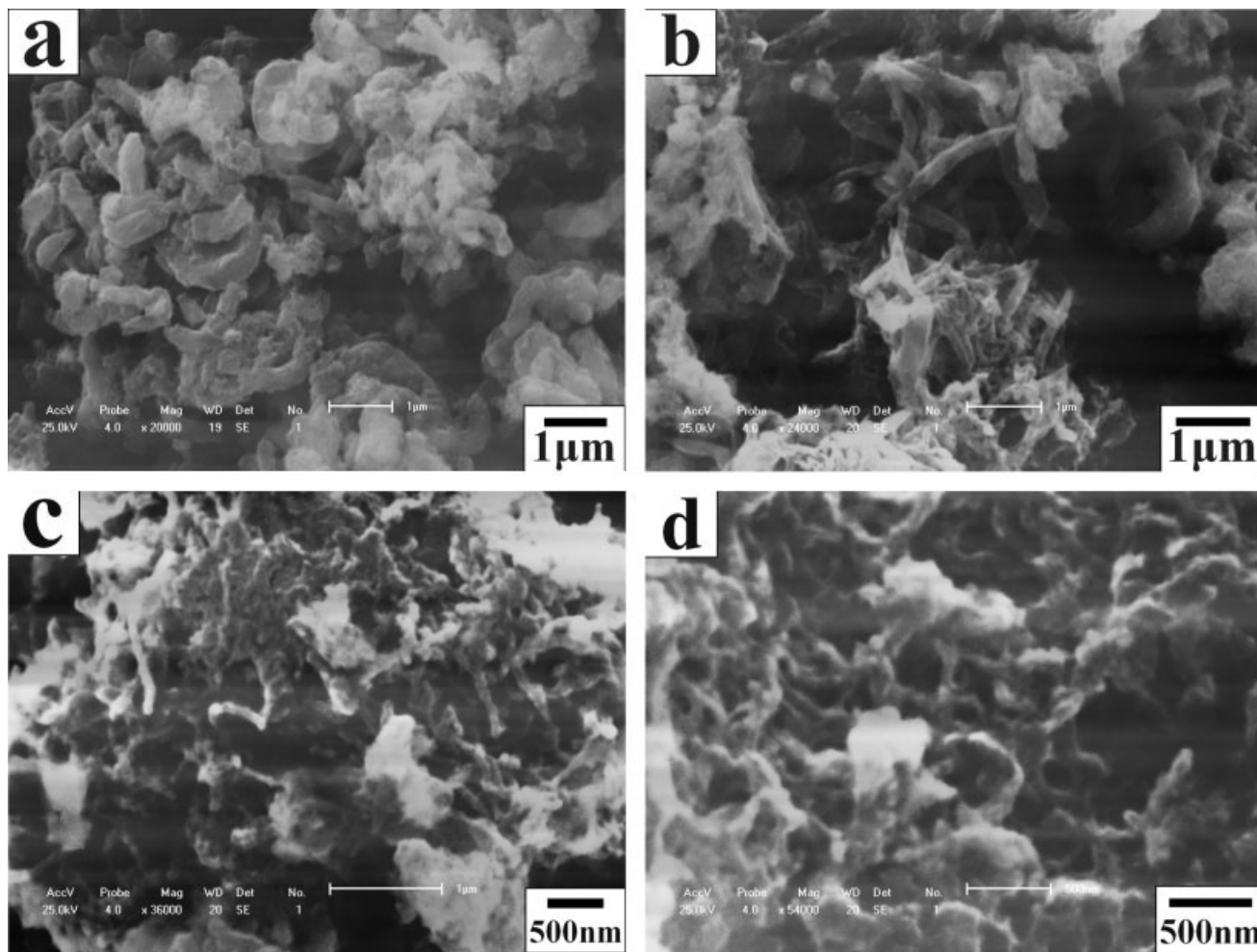


Figure 3 SEM images of PNMA/c-MWNT composites. (a) 1 wt % c-MWNTs; (b) 2 wt % c-MWNTs; (c) 3 wt % c-MWNTs; (d) 10 wt % c-MWNTs.

S/cm (Fig. 8). The lower room temperature conductivity of PNMA than PANI probably has something to do with its substituted group and low protonic acid

doping degree. Meanwhile, with the addition of 1 wt % c-MWNT into PNMA, the conductivities at room temperature increase from 1.4×10^{-6} S/cm to 3.9

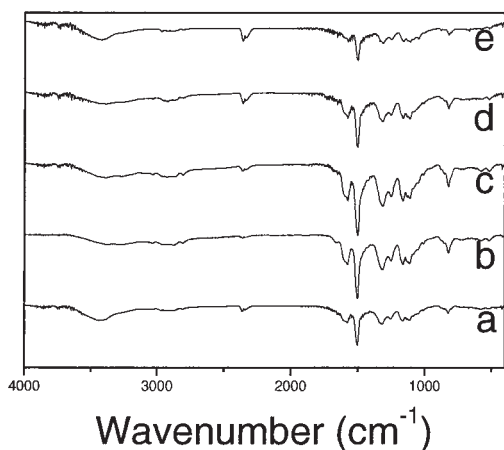


Figure 4 FTIR spectra of PNMA/c-MWNT composites. (a) 0 wt % c-MWNTs; (b) 1 wt % c-MWNTs; (c) 2 wt % c-MWNTs; (d) 5 wt % c-MWNTs; (e) 10 wt % c-MWNTs.

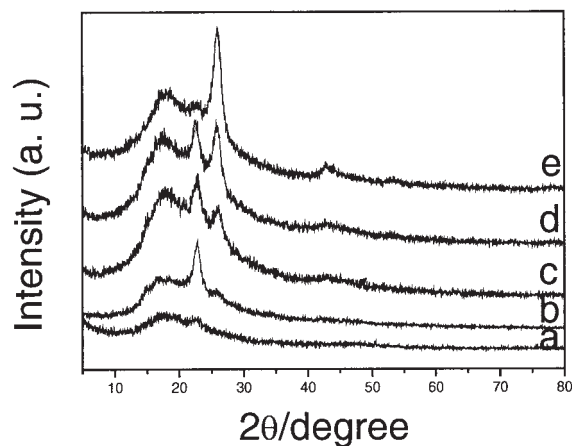


Figure 5 XRD patterns of PNMA/c-MWNT composites. (a) 0 wt % c-MWNTs; (b) 1 wt % c-MWNTs; (c) 2 wt % c-MWNTs; (d) 5 wt % c-MWNTs; (e) 10 wt % c-MWNTs.

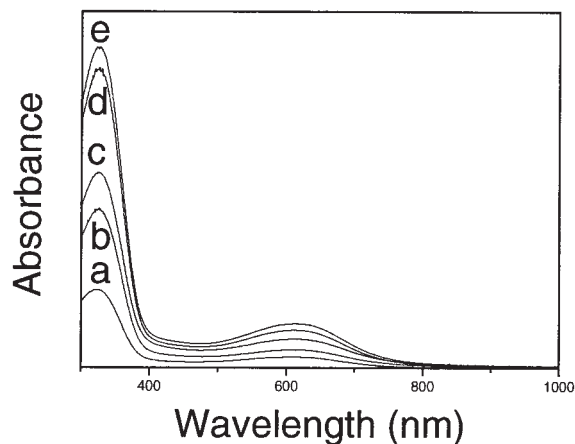


Figure 6 UV-vis spectra PNMA/c-MWNT composites in NMP solutions. (a) 0 wt % c-MWNTs; (b) 1 wt % c-MWNTs; (c) 2 wt % c-MWNTs; (d) 5 wt % c-MWNTs; (e) 10 wt % c-MWNTs.

$\times 10^{-6}$ S/cm. With the continuous increase in the content of c-MWNT, the conductivities at room temperature gradually increase from 3.9×10^{-6} S/cm for 1 wt % MWNT-containing PNMA/c-MWNT composites to 1.3×10^{-5} , 1.8×10^{-4} , 3.7×10^{-3} S/cm for 2 wt %, 5 wt %, and 10 wt % MWNT-containing PNMA/c-MWNT composites. The conductivity of PNMA/c-MWNT composites with 10 wt % c-MWNTs content at room temperature is 2600 times higher than that of PNMA without c-MWNTs. The reason is probably that c-MWNTs serve as a "conducting bridge" between the PNMA conducting domains, which increases the effective percolation.

CONCLUSIONS

We have described the synthesis of PNMA/c-MWNT composites with relatively high electrical conductivity.

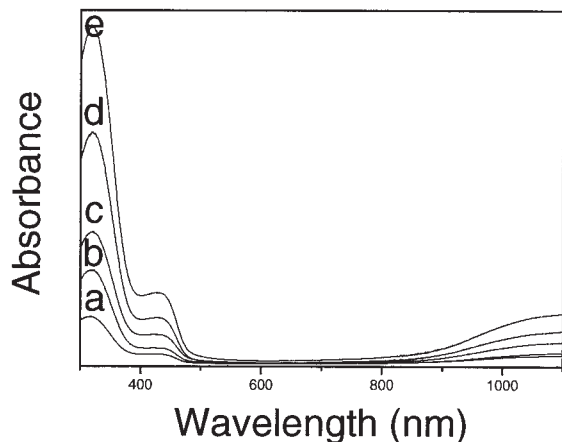


Figure 7 UV-vis spectra PNMA/c-MWNT composites in NMP solutions after adding one drop of 35% HCl solution. (a) 0 wt % c-MWNTs; (b) 1 wt % c-MWNTs; (c) 2 wt % c-MWNTs; (d) 5 wt % c-MWNTs; (e) 10 wt % c-MWNTs.

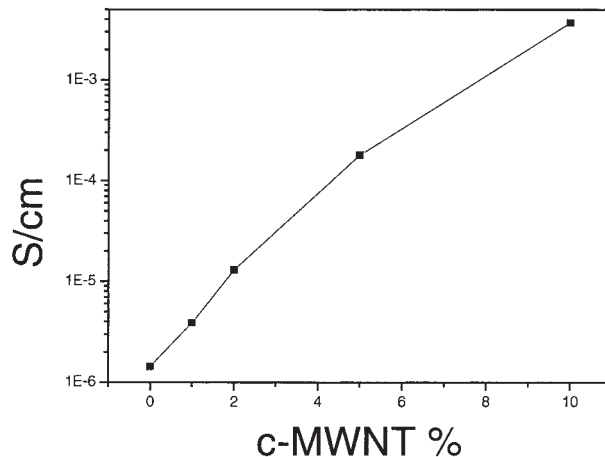


Figure 8 Room temperature conductivities of PNMA/c-MWNT composites with the fraction of c-MWNTs varying from 0 to 10%.

ity. The electrical conductivity at room temperature of 10 wt % c-MWNTs containing PNMA/c-MWNT composite is about 2600 times higher than that of PNMA without c-MWNTs. The morphology of PNMA/MWNT composites contains both the thinner fibrous phase and the larger block phase. It is presumed that c-MWNTs are used as a core in the formation of tubular shells of the fibrous PNMA/c-MWNT composites. FTIR, XRD, and UV-vis spectra are used to characterize the structure of PNMA/c-MWNT composites.

References

- Cao, Y.; Andreatta, A.; Heeger, A. J.; Smith, P. *Polymer* 1989, 30, 2305.
- Anderson, M. R.; Mattes, B. R.; Reiss, H.; Kaner, R. B. *Science* 1991, 252, 1412.
- Riul, A., Jr.; Soto, A. M. G.; Mello, S. V.; Bone, S.; Taylor, D. M.; Mattoso, L. H. C. *Synth Met* 2003, 132, 109.
- Saxena, V.; Malhotra, B. D. *Curr Appl Phys* 2003, 3, 293.
- Sharma, S. K.; Misra, S. C. K.; Tripathi, K. N. *J Nonlinear Opt Phys* 2003, 12, 39.
- Cao, Y.; Smith, P.; Heeger, A. J. *Synth Met* 1992, 48, 91.
- Kinlen, P. J.; Liu, J.; Ding, Y.; Graham, C. R.; Remsen, E. E. *Macromolecules* 1998, 31, 1735.
- Roy, B. C.; Gupta, M. D.; Bhoumik, L.; Ray, J. K. *Synth Met* 2002, 130, 27.
- Watanabe, A.; Mori, K.; Iwabuchi, A.; Iwasaki, Y.; Nakamura, Y. *Macromolecules* 1989, 22, 3521.
- Gupta, M. C.; Umare, S. S. *Macromolecules* 1992, 25, 138.
- Liao, Y. H.; Angelopoulos, M.; Levon, K. *J Polym Sci Part A: Polym Chem* 1995, 33, 2725.
- Storrier, G. D.; Colbran, S. B.; Hibbert, D. *Synth Met* 1994, 62, 179.
- Woo, H. S.; Czerw, R.; Webster, S.; Carroll, D. L.; Park, J. W.; Lee, J. H. *Synth Met* 2001, 116, 369.
- Chevalier, J. W.; Bergeron, J. Y.; Dao, L. H. *Macromolecules* 1992, 25, 3325.
- Comisso, N.; Daolio, S.; Mengoli, G.; Salmaso, R.; Zecchin, S.; Zotti, G. *J Electroanal Chem* 1988, 255, 97.

16. Barbero, C.; Miras, M. C.; Haas, O.; Kotz, R. J *Electroanal Chem* 1991, 310, 437.
17. Yano, J.; Kokura, M.; Ogura, K. *J Appl Electrochem* 1994, 24, 1164.
18. Athawale, A. A.; Kulkarni, M. V. *Sens Actuators* 2000, B67, 173.
19. Hao, Q. -L.; Kulikov, V.; Mirsky, V. M. *Sens Actuators* 2003, B94, 352.
20. Lindfors, T.; Ivaska, A. J. *Electroanal Chem* 2002, 535, 65.
21. de Heer, W.A.; Bonard, J. M.; Fauth, K.; Châtelain, A.; Forró, L.; Ugarte, D. *Adv Mater* 1997, 9, 87.
22. Baughman, R. H.; Spinks, G. M.; Wallace, G. G.; Mazzoldi, A.; de Kossi, D.; Rinzler, A. G.; Jaschinski, O.; Roth, S.; Kertesz, M. *Science* 1999, 284, 1340.
23. Sandler, J.; Schaffer, M.; Prasse, T.; Bauhofer, W.; Schulte, K.; Windle, A. H. *Polymer* 1999, 40, 5967.
24. Wei, C. Y.; Srivastava, D.; Cho, K. J. *Nano Lett* 2002, 2, 647.
25. Hughes, M.; Chen, G. Z.; Shaffer, M. S.; Fray, D. J.; Windle, A. H. *Chem Mater* 2002, 14, 1610.
26. Zhang, X. T.; Zhang, J.; Wang, R. M.; Liu, Z. F. *Carbon* 2004, 42, 1455.
27. Zhang, X. T.; Zhang, J.; Wang, R. M.; Zhu, T.; Liu, Z. F. *Chem-PhysChem* 2004, 5, 998.
28. Wu, T. M.; Lin, Y. W.; Liao, C. S. *Carbon* 2005, 43, 734.
29. Dai, L.; Lu, J.; Matthews, B.; Mau, W. H. *J Phys Chem B* 1998, 102, 4049.
30. Manohar, S. K.; MacDiarmid, A. G.; Cromack, K. R.; Ginder, J. M.; Epstein, A. J. *Synth Met* 1989, 29, E349.